Article

Does Core Size Matter in the Kinetics of Ligand Exchanges of Monolayer-Protected Au Clusters?

Rui Guo, Yang Song, Gangli Wang, and Royce W. Murray

J. Am. Chem. Soc., **2005**, 127 (8), 2752-2757• DOI: 10.1021/ja044638c • Publication Date (Web): 05 February 2005

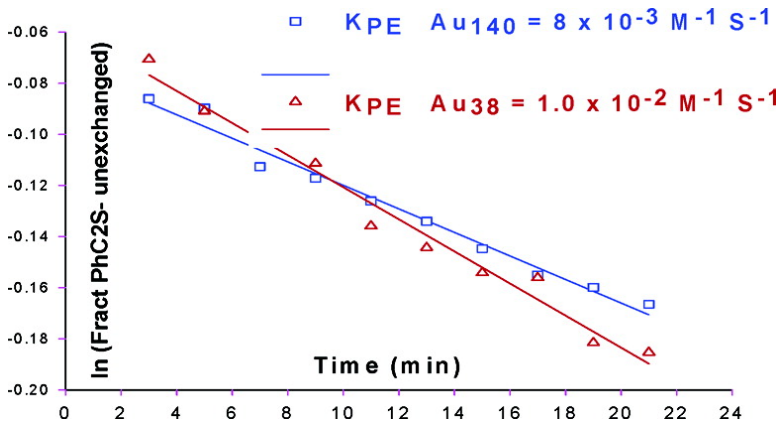

More About This Article

Additional resources and features associated with this article are available within the HTML version:

- Supporting Information
- Links to the 18 articles that cite this article, as of the time of this article download
- Access to high resolution figures
- Links to articles and content related to this article
- Copyright permission to reproduce figures and/or text from this article

View the Full Text HTML

J|A|C|S
ARTICLES
Published on Web 02/05/2005

Does Core Size Matter in the Kinetics of Ligand Exchanges of Monolayer-Protected Au Clusters?

Rui Guo, Yang Song,† Gangli Wang, and Royce W. Murray*

Contribution from the Kenan Laboratories of Chemistry, University of North Carolina, Chapel Hill, North Carolina 27599-3290

Received September 3, 2004; E-mail: rwm@email.unc.edu

Abstract: This paper compares the kinetics of exchanges of phenylethanethiolate ligands (PhC2S−) of the monolayer-protected clusters (MPCs) $Au_{38}(SC2Ph)_{24}$ and $Au_{140}(SC2Ph)_{53}$ with *p*-substituted arylthiols (*p*-X−PhSH), where X = NO_2, Br, CH_3, OCH_3, and OH. First-order rate constants at 293 K for exchange of the first ca. 25% of the ligands on the molecule-like $Au_{38}(SC2Ph)_{24}$ MPC, measured using ^{1}H NMR, vary linearly with the in-coming arythiol concentration; ligand exchange is an overall second-order reaction. Remarkably, the second-order rate constants for ligand exchange on $Au_{38}(SC2Ph)_{24}$ are very close to those of corresponding exchange reactions on the larger nanoparticle $Au_{140}(SC2Ph)_{53}$ MPCs. These are the first results that quantitatively show that the chemical reactivity of different sized nanocrystals is almost independent of size; presumably, this is because the locus of the initial ligand exchanges is a common kind of site, thought to be the nanocrystal vertexes. The rates of later stages of exchange (beyond ca. 25%) differ for Au_{38} and Au_{140} cores, the latter being much slower presumably due to its larger terrace-like surface atom content. The reverse exchange reaction was studied for Au_{38}(*p*-X−arylthiolate)$_{24}$ MPCs (X = NO_2, Br, and CH_3), where the in-coming ligand is now phenylethanethiol. Remarkably, the rate constants of both forward and reverse exchanges display identical substituent effects, which implies a concurrent bonding of both in-coming and leaving ligands to the Au core in the rate-determining step, as in an associative mechanism. X = NO_2 gives the fastest rates, and the ratio of forward and reverse rate constants gives an equilibrium constant of $K_{EQ,PE}$ = 4.0 that is independent of X.

Introduction

Monolayer-protected metal clusters (MPCs) are nanoparticles coated with dense, protecting monolayers of organothiolate,[1−4] organophosphine,[5−7] or organoamine ligands.[8] Thiolate ligands are used widely for MPCs with Au cores. One vital aspect of MPCs is that their chemical properties can be manipulated by varying the monolayer with ligand place-exchange reactions,[4,8−22] as we showed for thiolate ligands on Au nanoparticles some time ago.[23]

The electrochemical properties of MPCs are known[24−28] to be core-size dependent, but whether their ligands exhibit size-dependent chemical reactivity has not been established. An important aspect of Au nanoparticle surface chemistry is that their surfaces are not uniform, but nanocrystalline, and accordingly contain a diversity of ligand binding sites: vertexes, edges, and terraces. These different locations on the nanoparticle surface can have different electron densities[29] and steric accessibilities that potentially lead to equilibrium binding

† Present address: Milliken & Co., Spartanberg, SC.

(1) Templeton, A. C.; Wuelfing, W. P.; Murray, R. W. *Acc. Chem. Res.* **2000**, *33*, 27.
(2) Whetten, R. L.; Shafigullin, M. N.; Khoury, J. T.; Schaaff, T. G.; Vezmar, I.; Alvarez, M. M.; Wilkinson, A. *Acc. Chem. Res.* **1999**, *32*, 397.
(3) Brust, M.; Walker, M.; Bethell, D.; Schiffrin, D. J.; Whyman, R. *J. Chem. Soc., Chem. Commun.* **1994**, 801.
(4) Brown, L. O.; Hutchison, J. E. *J. Am. Chem. Soc.* **1997**, *119*, 12384.
(5) Schmid, G. *Chem. Rev.* **1992**, *92*, 1709.
(6) Weare, W. W.; Reed, S. M.; Warner, M. G.; Hutchison, J. E. *J. Am. Chem. Soc.* **2000**, *122*, 12890.
(7) Petroski, J.; Chou, M. H.; Creutz, C. *Inorg. Chem.* **2004**, *43*, 1597.
(8) Brown, L. O.; Hutchison, J. E. *J. Am. Chem. Soc.* **1999**, *121*, 882.
(9) Song, Y.; Murray, R. W. *J. Am. Chem. Soc.* **2002**, *124*, 7096.
(10) Hostetler, M. J.; Templeton, A. C.; Murray, R. W. *Langmuir* **1999**, *15*, 3782.
(11) Kell, A. J.; Stringle, D. L. B.; Workentin, M. S. *Org. Lett.* **2000**, *2*, 3381.
(12) Han, L.; Daniel, D. R.; Maye, M. M.; Zhong, C.-J. *Anal. Chem.* **2001**, *73*, 4441.
(13) Kell, A. J.; Workentin, M. S. *Langmuir* **2001**, *17*, 7355.
(14) Wuelfing, W. P.; Zamborini, F. P.; Templeton, A. C.; Wen, W.; Yoon, H.; Murray, R. W. *Chem. Mater.* **2001**, *13*, 87.
(15) Ionita, P.; Caragheorgheopol, A. *J. Am. Chem. Soc.* **2002**, *124*, 9048.
(16) Lin, S.-Y.; Liu, S.-W.; Lin, C.-M.; Chen, C. *Anal. Chem.* **2002**, *74*, 330.
(17) Wuelfing, W. P.; Murray, R. W. *J. Phys. Chem. B* **2002**, *106*, 3139.
(18) Zamborini, F. P.; Leopold, M. C.; Hicks, J. F.; Kulesza, P. J.; Malik, M. A.; Murray, R. W. *J. Am. Chem. Soc.* **2002**, *124*, 8958.
(19) Lee, D.; Donkers, R. L.; DeSimone, J. M.; Murray, R. W. *J. Am. Chem. Soc.* **2003**, *125*, 1182.
(20) Li, D.; Li, J. *Surf. Sci.* **2003**, *522*, 105.
(21) Pengo, P.; Broxterman, Q. B.; Kaptein, B.; Pasquato, L.; Scrimin, P. *Langmuir* **2003**, *19*, 2521.
(22) Woehrle, G. H.; Warner, M. G.; Hutchison, J. E. *J. Phys. Chem. B* **2002**, *106*, 9979.
(23) Hostetler, M. J.; Green, S. J.; Stokes, J. J.; Murray, R. W. *J. Am. Chem. Soc.* **1996**, *118*, 4212.
(24) Chen, S.; Ingram, R. S.; Hostetler, M. J.; Pietron, J. J.; Murray, R. W.; Schaaff, T. G.; Khoury, J. T.; Alvarez, M. M.; Whetten, R. L. *Science* **1998**, *280*, 2098.
(25) Hicks, J. F.; Miles, D. T.; Murray, R. W. *J. Am. Chem. Soc.* **2002**, *124*, 13322.
(26) Lee, D.; Donkers, R. L.; Wang, G.; Harper, A. S.; Murray, R. W. *J. Am. Chem. Soc.* **2004**, *126*, 6193.
(27) Jimenez, V. L.; Georganopoulou, D. G.; White, R. J.; Harper, A. S.; Mills, A. J.; Lee, D.; Murray, R. W. *Langmuir* **2004**, *20*, 6864.
(28) Yang, Y.; Chen, S. *Nano Lett.* **2003**, *3*, 75.
(29) (a) Häkkinen, H.; Barnett, R. N.; Landman, U. *Phys. Rev. Lett.* **1999**, *82*, 3264. (b) Häberlen, O. D.; Chung, S.-C.; Stener, M.; Rösch, N. *J. Chem. Phys.* **1997**, *106*, 5189.

10.1021/ja044638c CCC: $30.25

thermodynamics and ligand exchange kinetics that vary for different core sites. This mix of chemical properties depends on the MPC core size; for smaller cores, the fraction of atoms that lie on vertex and edge sites increases relative to terrace sites. The vertex and edge sites are called "defect sites"; analogous sites in self-assembled monolayers (2D SAMs) on flat Au surfaces[30] lie at step edges and grain boundaries and also the more numerous boundaries of ordered monolayer domains. It is well-accepted[30] that such defect sites exhibit a higher reactivity toward thiolate exchange than do intra-domain Au(111) terrace sites.

The ligand exchange kinetics of alkanethiolate-coated Au MPCs with average core diameters 1.6 and 2.2 nm, and corresponding average compositions $Au_{140}(ligand)_{53}$ and $Au_{314}(ligand)_{91}$, have been investigated[9,10] using ^{1}H NMR, finding that: (a) the exchange reactions with substituted alkanethiols follow a 1:1 stoichiometry, releasing one out-going ligand as a thiol from the MPC monolayer for every newly bound in-coming thiolate, in a second-order process that was interpreted as an associative reaction, (b) disulfides or oxidized sulfur species are not involved, (c) the exchange rate is accelerated if the core is made electron-deficient (as by oxidative charging), and (d) the exchange rate is initially rapid but then slows dramatically. The rate profile was interpreted[9,10] as reflecting high kinetic reactivity of vertex and edge sites relative to low kinetic reactivity of terrace-like core surface sites. The last point is supported by more recent results[31] for $Au_{140}(SC2Ph)_{53}$ (1.6 nm core diam) MPCs reacting with substituted thiophenols, where, after the initial (5−8) ligand exchanges (again in a second-order process), there was a gradual and then near-cessation of the reaction rate (over days) at <50% exchange of the original ligands. Besides reflecting large differences in reactivity of defect versus terrace-like sites for ligand exchange, these results require that ligand surface migration between different kinds of sites is a relatively slow process.

The present study was prompted by an interest in the extent to which ligand exchange dynamics depend on the MPC core size. Previous ligand exchange investigations were not designed with an eye to effects of core size. $Au_{140}(SC2Ph)_{53}$ and $Au_{38}(SC2Ph)_{24}$ MPCs are anticipated from theoretical studies[29a] to have truncated octahedral nanocrystalline shapes in which the nanocrystals have 96 and 32 surface atoms, respectively. The number of vertex atom sites is the same on the two cores, but their proportion is far greater for the Au_{38} core. The electronic properties also differ; the Au_{140} core is metal-like (no HOMO−LUMO gap has been detected), and its electrochemical properties in electrolyte solutions are dominated by charging effects called "quantized double layer" (QDL) charging.[25] The Au_{38} core, in contrast, is molecule-like, displaying a HOMO−LUMO gap[26] of about 1.3 eV. The former has a more-or-less uniform (although perhaps thin) continuum of electronic states, while electron density in the latter has collapsed to definable molecular orbitals. Are these differences in electronic structure reflected in ligand reactivity differences, even if the reaction occurs at the same kind of core surface site? We will show here that at least for the ligand exchange dynamics of the early-exchanging, presumably vertex sites, the ligand exchange rates for SC2Ph-coated Au_{38} and Au_{140} cores with substituted thiophenols are very similar.

Another result of the present study is that the different proportions of defect versus terrace sites for Au_{38} versus Au_{140} cores lead to different ligand exchange reaction profiles for the later-exchanging ligands. The Au_{38} exchange rate continues with a modest diminution in rate; that for Au_{140} shows a drastic slowing. Additionally, that nearly 100% exchange can be accomplished for $Au_{38}(SC2Ph)_{24}$ MPCs allows isolation of $Au_{38}(SPhX)_{24}$ exchange products, and subsequent inspection of the rate of the reverse exchange reaction. The reverse exchange displays a nearly identical substituent effect and allows estimation of the (initial) ligand exchange equilibrium constant.

Previous ligand exchanges[9,10] followed by batch reaction/quenching procedures were replaced by a continuous ^{1}H NMR method in our most recent study.[31] An analogous method was used here because it allows collection of more detailed kinetic data. Detailed kinetic profiles are also made possible[30g] by use of release of fluorophores from MPC surfaces (where their emissions are quenched) upon exchange, and by EPR observations[33−35] of spin-labeled ligands before and after binding to MPCs. Exchange reaction[30g] of a large excess of decanethiol with a 4 nm diameter MPC coated with thiolated pyrene ligands led to complete exchange and fractional reaction orders in the in-coming thiol. Reaction of butanethiolate-protected 2.6 nm diameter MPCs with disulfides functionalized with a spin label[33−35] resulted in exchange of only 4−6 of the ca. 150 −SC4 ligands present, with a roughly zero-order dependence on disulfide concentration, and pronounced exchange-kinetics effects associated with aging[35] of the butanethiolate nanoparticles. (Such aging effects, potentially associated with surface-reorganizational behavior[30f] of butanethiolate ligands, have not been observed by us for either $Au_{140}(SC2Ph)_{53}$ or $Au_{38}(SC2Ph)_{24}$ MPCs.) The chemical nature of our and these other MPC exchange reactions, and those reported on flat Au surfaces,[30] are so diverse as to make comparisons of them tenuous at this juncture of the field.

Experimental Section

Chemicals. 4-Nitrothiophenol (ACROS, 95%), *p*-toluenethiol (ACROS, 98%), 4-methoxybenzenethiol (ACROS, 98%), phenylethylthiol (PhC2SH, Aldrich, 98%), 4-bromothiophenol (Aldrich, 95%), 4-mercaptophenol (Aldrich, 90%), *tetra-n*-octylammonium bromide (Oct_4NBr, Fluka, 98%), sodium borohydride (Aldrich, 99%), toluene (Fisher), and d_2-methylene chloride (Cambridge Isotope Laboratories, Inc.) were all used as received. Hydrogen tetrachloroaurate trihydrate (from 99.999% pure gold) was prepared by a literature procedure[36] and stored in a freezer at −20 °C. A Millipore Nanopure water purification system was used to obtain low conductivity water.

(30) (a) Collard, D. M.; Fox, M. A. *Langmuir* **1991**, *7*, 1192. (b) Kolega, R. R.; Schlenoff, J. B. *Langmuir* **1998**, *14*, 5469. (c) Lin, P. H.; Guyot-Sionnest, P. *Langmuir* **1999**, *15*, 6825. (d) Chidsey, C. E. D.; Bertozzi, C. R.; Putvinski, T. M.; Mujsce, A. M. *J. Am. Chem. Soc.* **1990**, *112*, 4301. (e) Bain, C. D.; Troughton, E. B.; Tao, Y.-T.; Evall, J.; Whitesides, G. M.; Nuzzo, R. G. *J. Am. Chem. Soc.* **1989**, *111*, 321. (f) Hutt, D. A.; Leggett, G. J. *Langmuir* **1997**, *13*, 3055. (g) Montalti, M.; Prodi, L.; Zaccheroni, N.; Baxter, R.; Teobaldi, G.; Zerbetto, F. *Langmuir* **2003**, *19*, 5172−5174.

(31) Donkers, R. L.; Song, Y.; Murray, R. W. *Langmuir* **2004**, *20*, 4703.

(32) For the purpose of comparisons, the 40% segment was dictated by the practical fact that beyond 40%, ligand exchange for $Au_{140}(SC2Ph)_{53}$ exhibits a continued slowing. A plot of Figure 3b at even longer times becomes curved and eventually almost flat, signaling a near-cessation of the reaction rate.

(33) (a) Ionita, P.; Caragheorgheopol, A.; Gilbert, B. C.; Chechik, V. *J. Am. Chem. Soc.* **2002**, *124*, 9048. (b) Ionita, P.; Caragheorgheopol, A.; Gilbert, B. C.; Chechik, V. *Langmuir* **2004**, *20*, 11536−11544.

(34) Chechik, V.; Wellsted, H. J.; Korte, A.; Gilbert, B. C.; Caldararu, H.; Ionita, P.; Caragheorgheopol, A. *Faraday Discuss.* **2004**, *125*, 279.

(35) Chechik, V. *J. Am. Chem. Soc.* **2004**, *126*, 7780.

(36) *Handbook of Preparative Inorganic Chemistry*; Brauer, G., Ed.; Academic Press: New York, 1965; p 1054.

Table 1. Summary of Phase I Pseudo-First-Order Rate Constants for Ligand Exchange Reactions of Different *p*-Substituted Arylthiols with 2.8×10^{-4} M $Au_{38}(SC2Ph)_{24}$ MPCs

$[NO_2PhSH]^a$ (M)	k_{obs} (s^{-1}) $\times 10^{-4}$	$[BrPhSH]^a$ (M)	k_{obs} (s^{-1}) $\times 10^{-4}$	$[CH_3PhSH]^a$ (M)	k_{obs} (s^{-1}) $\times 10^{-4}$	$[OCH_3PhSH]^a$ (M)	k_{obs} (s^{-1}) $\times 10^{-4}$
0.0089	1.02 ± 0.06	0.0201	0.64 ± 0.04	0.0272	0.49 ± 0.03	0.0126	0.32 ± 0.02
0.0185	1.75 ± 0.09	0.0309	1.05 ± 0.05	0.0378	0.64 ± 0.04	0.0202	0.51 ± 0.03
0.0234	2.28 ± 0.11	0.0395	1.41 ± 0.10	0.0485	0.77 ± 0.03	0.0265	0.63 ± 0.04
0.0280	2.80 ± 0.14	0.0435	1.48 ± 0.10	0.0590	0.91 ± 0.06	0.0399	0.91 ± 0.06

[a] The rate constants for several test reactions using deuteriothiol, *p*-X−PhSD, were within experimental error the same as those for *p*-X−PhSH; that is, no kinetic isotope effect is present.

Synthesis of *p*-X−PhSD Thiols. *p*-X−PhSD thiols used to test for kinetic isotope effect (none found, see Table 1) were synthesized as previously described.[31] Briefly, for X = NO_2, Br, CH_3, and OCH_3 thiols, 3 mL of D_2O was vigorously stirred with ca. 100 mg of thiol/3 mL of CD_2Cl_2 for 24 h. The organic layer was separated, dried over sodium sulfate, filtered, and rotary evaporated. Complete loss of the SH NMR signal in dry CD_2Cl_2 showed complete D/H exchange; the deuterated thiols were used immediately after being characterized.

Synthesis of $Au_{38}(SC2Ph)_{24}$. $Au_{38}(SC2Ph)_{24}$ was synthesized as described before.[37] Briefly, in a two-phase Brust[3] synthesis, hydrogen tetrachloroaurate (3.1 g, 11.1 mmol) was phase-transferred into toluene with Oct_4NBr, followed by addition of a 3-fold molar excess (relative to Au) of phenylethylthiol, forming a gold(I)−thiol polymer. This was reduced by rapidly adding a 10-fold excess of aqueous $NaBH_4$ at 0 °C, vigorously stirring the solution at 0 °C for 20 h. After the bottom aqueous layer was removed, the toluene was rotary-evaporated at room temperature and the $Au_{38}(SC2Ph)_{24}$ was extracted from the crude product with acetonitrile. The dried product was washed copiously with methanol until mostly cleaned of Oct_4N^+ cation (the residue is ≤1 Oct_4N^+ per MPC according to ^{1}H NMR). The product was characterized by ^{1}H NMR (Figure S-1) and UV−vis spectra as was previously done.[31]

Ligand Exchange Kinetics by ^{1}H NMR Spectroscopy. ^{1}H NMR spectra of (not degassed) solution mixtures of $Au_{38}(SC2Ph)_{24}$ (6.0 mg/2.0 mL after mixing) and *p*-X−PhSH ligands (amounts varied based upon desired reactant ratios) in CD_2Cl_2 were collected with a Bruker AC500 spectrometer at 293 K. Ferrocene (sublimed, typically 0.6 mg/2.0 mL after mixing) served as an internal standard. Briefly, after a ^{1}H NMR spectrum of the initial solution (1 mL) of ferrocene and *p*-X−PhSH was acquired, it was rapidly mixed with the MPC solution (6.0 mg/1 mL) and placed in the pre-shimmed spectrometer for repetitive collection of 1−9 ppm (vs TMS) spectra, using a 17 s acquisition time per spectrum and a time interval between spectra of 2 min. $\mathbf{T}_1$ was set at 1 s instead of 0 s as was done in the $Au_{140}(SC2Ph)_{53}$ case.[31] The ca. 2.8 ppm quartet resonance originates exclusively from the liberated phenylethanethiol (HS−***CH$_2$***−CH_2Ph), which was used to monitor the extent of the exchange reaction; its growth relative to the ferrocene standard is illustrated in Figure 1. The % exchanged PhC2S− from the $Au_{38}(SC2Ph)_{24}$ nanoparticle is the percentage of liberated phenylethanethiol versus the initial 24 phenylethanethiolate ligands of the nanoparticle. The previously[31] reported rates of ligand exchange for $Au_{140}(SC2Ph)_{53}$ were measured by a different procedure and are remeasured using the above procedure at 293 K, for a more rigorous comparison with the $Au_{38}(SC2Ph)_{24}$ data. Rest potentials of $Au_{38}(SC2Ph)_{24}$ and $Au_{140}(SC2Ph)_{53}$ solutions correspond to a $MPC^{0/+1}$ mixture and are substantially unchanged after ligand exchanges of 3 h. The previously observed[9,10] effects of changing the core charge and of dioxygen were not investigated in this study. In measurements of the reverse exchange reaction, the singlet from liberated ***H***S−Ph−X was monitored to follow the extent of exchange.

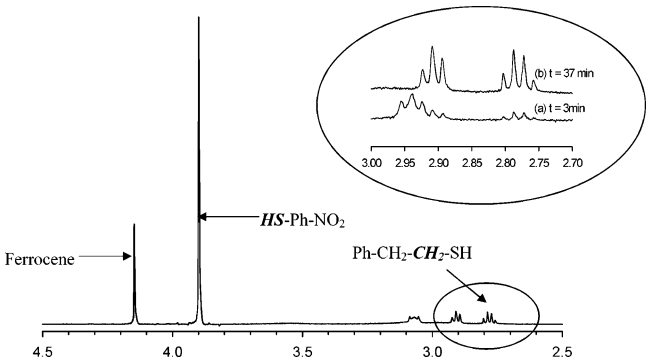

Figure 1. ^{1}H NMR spectra for the exchange of phenylethanethiolate (PhC2S−) by 4-nitrothiophenol (4-NO_2−PhSH) onto $Au_{38}(SC2Ph)_{24}$ at 293 K. Inset: (a) at $t = 3$ min; (b) at $t = 37$ min. Ferrocene serves as internal standard. The integrated 2.8 ppm quartet signal, representing α-CH_2 on liberated phenylethanethiol (HS−***CH$_2$***−CH_2−Ph), is used for the kinetic measurement. The α-CH_2 resonance on bound phenylethanethiolate, a broad peak at ca. 3.35 ppm (Figure S-1), is somewhat suppressed in this spectrum. The ca. 2.9 ppm peaks are from β-CH_2 on bound phenylethanethiolate (−S−CH_2−***CH$_2$***−Ph) and liberated phenylethanethiol (HS−CH_2−***CH$_2$***−Ph); the ca. 3.1 ppm triplet is from the α-proton of $(Oct_4)NBr$ salt impurity (ca. one Oct_4^+ cation per MPC; the kinetic influence of a single potentially associated adsorbed bromide ion should be small).

Results and Discussion

Ligand Exchange Kinetics. The previous[31] NMR approach to ligand exchange dynamics of $Au_{140}(SC2Ph)_{53}$ (using $T_1 = 0$ relaxation delay pulse to effectively suppress signals from Au_{140} MPC-bound thiolate ligands) failed in the present case because the sharper resonances for Au_{38} ligands were not similarly suppressed. The ligand exchange was instead followed using the α-CH_2 ca. 2.8 ppm quartet resonance of phenylethanethiol liberated from the $Au_{38}(SC2Ph)_{24}$ monolayer by exchange with *p*-X−PhSH thiols. Figure 1 illustrates the monitoring scheme; although the quartet signal is initially small, it is well resolved from resonances from Au_{38}-bound phenylethanethiolate ligands at ca. 2.9 ppm (triplet) and at 3.35 ppm (broad, see Figure S-1). No signals suggestive of disulfides or other oxidized forms of organic sulfur were observed, as was the case previously.[9,10,31]

Kinetic results for exchange with in-coming ligand *p*-NO_2−PhSH are shown in Figure 2 for $Au_{38}(SC2Ph)_{24}$ (curve a) and $Au_{140}(SC2Ph)_{53}$ (curve b), converting the NMR peak integrals into percentages of phenylethanethiolate ligands exchanged. The kinetic profile for the $Au_{140}(SC2Ph)_{53}$ MPC is very similar to the previous report;[31] the initially rapid reaction slows down dramatically and comes to an apparent near-halt after 40−50% of the PhC2S-monolayer is replaced. In contrast, the $Au_{38}(SC2Ph)_{24}$ MPC exchange reaction continues within the time frame of Figure 2a to replace 75% of the monolayer. (Figure S-2 shows the kinetic profile with the *Y*-axis both in %PhC2S-exchanged and in number of ligands exchanged.)

(37) Donkers, R. L.; Lee, D. L.; Murray, R. W. *Langmuir* **2004**, *20*, 1945.
(38) Lowry, T. H.; Richardson, K. S. *Mechanism and Theory in Organic Chemistry*, 3rd ed.; Harper & Row: New York, 1987.

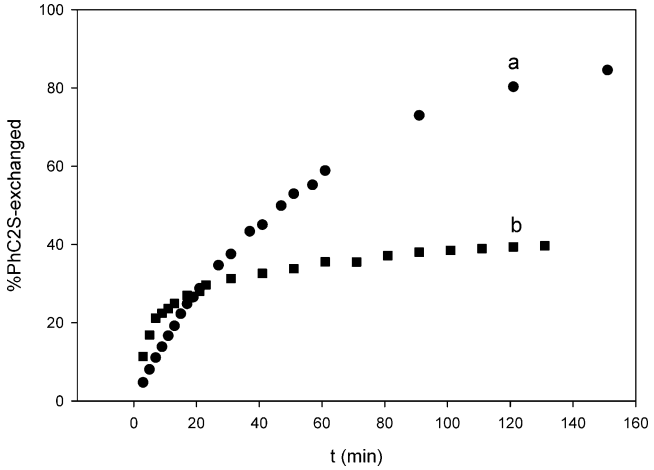

Figure 2. Reaction profile for exchange of phenylethanethiolate (PhC2S−) by *p*-nitrothiophenol (NO_2PhSH) onto (a) $Au_{38}(SC2Ph)_{24}$ and (b) $Au_{140}(SC2Ph)_{53}$ at mole ratios of NO_2PhSH/PhC2S− = 4.2:1 and 1.3:1, respectively. MPC concentration is 2.8×10^{-4} M in both cases and at the same temperature of 293 K. A more detailed version of this figure is in the Supporting Information.

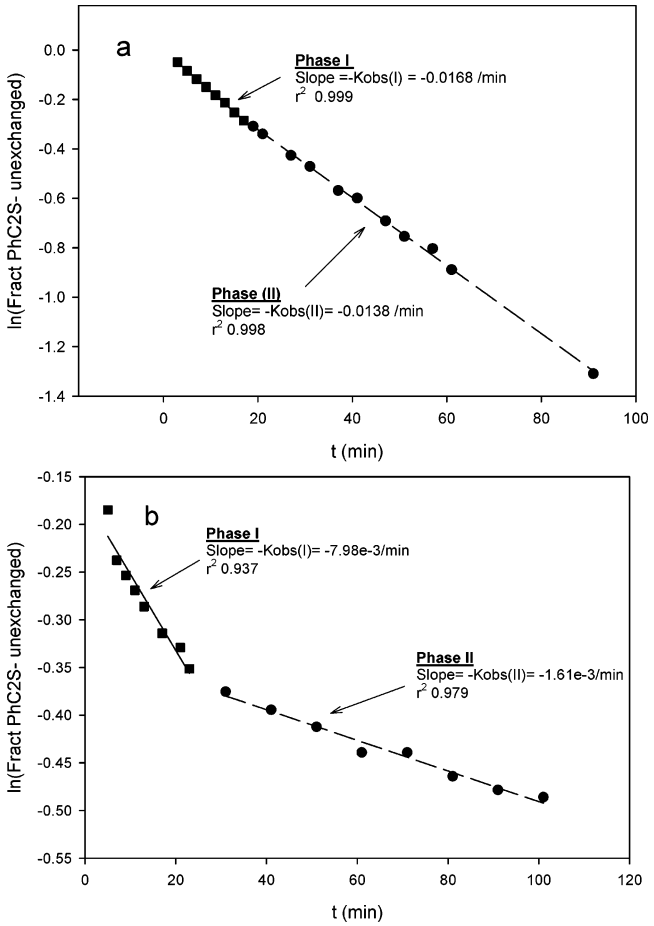

Figure 3. (a) Pseudo-first-order rate plots for exchange of phenylethanethiolate (PhC2S−) by *p*-nitrothiophenol (NO_2PhSH) onto (panel a) $Au_{38}(SC2Ph)_{24}$ and (panel b) $Au_{140}(SC2Ph)_{53}$, at mole ratios of NO_2PhSH/PhC2S− = 4.2:1 and 1.3:1, respectively. In the plots, Phase I corresponds to exchange of the initial ca. 25% of the PhC2S-monolayer and Phase II to ca. 80% and 40% of the PhC2S-monolayer in panels a and B, respectively.

Figure 3 shows a first-order rate analysis of the kinetic profiles of Figure 2. Both reactions are roughly biphasic, a more rapid first-order process transitioning to a slower first-order process. This signals serial first-order reactions in which the second,

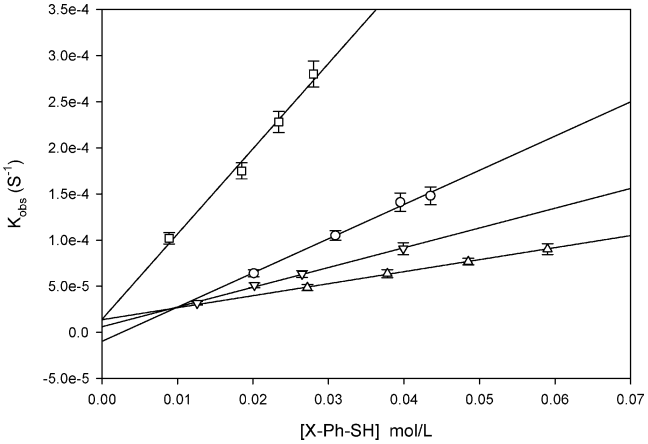

Figure 4. Second-order rate plot for reaction of 2.8×10^{-4} M $Au_{38}(SC2Ph)_{24}$ with in-coming ligands (□) $HSPhNO_2$, (○) HSPhBr, (△) $HSPhCH_3$, and (▽) $HSPhOCH_3$. *Y*-intercepts are zero within experimental error.

slower (Phase II) reaction becomes dominant when the participants in the faster first reaction (Phase I) are exhausted. We use the designation of Phase I to represent exchange of the first ca. 25% of the PhC2S− ligands by *p*-NO_2−PhSH, and Phase II to represent[32] the ensuing exchanges. For $Au_{38}(SC2Ph)_{24}$ MPCs, the Phase II rate constants are only ca. 20% smaller than those in Phase I, whereas for $Au_{140}(SC2Ph)_{53}$ the Phase II rates are 4−5-fold smaller. This pattern of differences in Phase I versus Phase II rates for the two MPCs was observed for the kinetics of all three *p*-substituted arylthiols (X = NO_2, Br, and CH_3), even though the rates for both MPCs decreased concurrently by ca. 4−6-fold through the series of in-coming ligands. Interpretation of these observations is deferred to below.

The $Au_{38}(SC2Ph)_{24}$ ligand exchange by *p*-substituted arylthiols was also first-order for X = Br, CH_3, OCH_3, and OH, and Phase I and Phase II behavior was again seen (Supporting Information, Figures S-3, S-4). Further, first-order behavior was established for X = NO_2, Br, CH_3, and OCH_3 for different in-coming thiol concentrations (Table 1); plots of the Phase I results are shown in Figure 4. Figure 4 demonstrates an overall second-order behavior; the plots are linear with intercepts within ca. $\pm 2 \times 10^{-5}$ s^{-1} of the origin. (The nonzero intercept seen[31] for X = NO_2 in the previous $Au_{140}(SC2Ph)_{53}$ study was not encountered for $Au_{38}(SC2Ph)_{24}$.) The second-order rate constants ($K_{PE(I)}$) taken from the slopes of Figure 4 (Phase I of the reaction) are summarized in Table 2. The Phase II first-order rate constants were also established to vary linearly with in-coming ligand concentration for the case of X = NO_2 (Figure S-5); the $K_{PE(II)}$ results given in Table 2 for the other *p*-substituted arylthiols assume their corresponding second-order behavior.

The first interpretation that can be given the $K_{PE(I)}$ data in Table 2 is that the second-order reaction, first-order each in MPC (and independent of initial MPC concentration; see table footnote) and in-coming ligand, is consistent with an associative ligand exchange mechanism as proposed previously[9,10,31] for larger core Au_{314} and Au_{140} MPCs. It is worth mentioning that first-order rate dependence on MPC and in-coming thiol concentrations does not by itself prove an associative process, because it is possible to write mechanisms including a rapid equilibrium pre-dissociation of monolayer ligands that show the same reaction order. The associative interpretation is, however,

Table 2. Second-Order Rate Constants of Ligand Exchange Reaction of Gold Nanoparticles $Au_{38}(SC2Ph)_{24}$ and $Au_{140}(SC2Ph)_{53}$ with Different *p*-Substituted Arylthiols (*p*-XPhSH)

MPCs	in-coming ligand	in-coming ligand:PhC2[a]	$k_{PE(I)}$[b] (10^{-3} M^{-1} s^{-1})	in-coming ligand:PhC2[a]	$k_{PE(II)}$[c] (10^{-3} M^{-1} s^{-1})
$Au_{38}(SC2Ph)_{24}$[d]	NO_2PhSH	(1.3−4.2):1	10.1 ± 0.6	4.2:1	8.5
	BrPhSH	(3.1−6.7):1	3.4 ± 0.3	6.7:1	1.8
	CH_3PhSH	(4.3−9.3):1	1.6 ± 0.2	4.3:1	1.1
	CH_3OPhSH	(1.8−6.0):1	2.4 ± 0.3	4.0:1	1.3
	HOPhSH	7.1:1	2.3	7.1:1	1.0
$Au_{140}(SC2Ph)_{53}$[d,e]	NO_2PhSH	1.3:1	7.8	1.3:1	1.7
	BrPhSH	2.2:1	2.2	2.2:1	0.6
	CH_3PhSH	3.3:1	1.8	3.3:1	0.6

[a] The relative number of moles of in-coming arylthiols and the original phenylethanethiolate ligands in the monolayers of the $Au_{38}(SC2Ph)_{24}$ and $Au_{140}(SC2Ph)_{53}$ MPCs. [b] Average second-order rate constants of Phase I (ca. 25% of the PhC2S-thiolate is exchanged), for *p*-substituted X = NO_2, Br, CH_3, OCH_3. For X = OH, $k_{PE(I)}$ is taken from a single in-coming ligand concentration, and second-order is assumed. For X = NO_2 and Au_{38}, the same second-order constant for both reaction phases was obtained when the initial MPC concentration used was ca. 3-fold larger. [c] Second-order rate constants of Phase II calculated from results at a single in-coming ligand concentration. [d] The MPC solutions, judging from electrochemical rest potentials, contained roughly equal amounts of Au^0 and Au^{1+} cores. [e] The previous[31] Phase I results for X = NO_2, Br, and CH_3 were $K_{PE(I)} = 14$, 6.4, and 4.3×10^{-3} M^{-1} s^{-1}, respectively, which differ by factors of 2−3-fold from the present results. Considering that different NMR procedures were used, and the potential variability among the monodispersity of Au_{140} nanoparticle synthetic preparations by different workers, we regard this level of agreement as acceptable. Phase II was not assessed in the previous work.

more firmly supported by a comparison of reverse versus forward exchange reactions as discussed later. Second, the rate of phenylethanethiolate ligand exchange by thiolates of *p*-X−PhSH varies with the nature of X; that is, there is a substituent effect on the reaction rate. This was also observed in the Au_{140} study[31] and shows explicitly that the in-coming ligand is involved in the rate-controlling step of the exchange, further supporting an associative process.

The third and perhaps most significant observation taken from Table 2 is that the rate constants for Phase I ligand exchange are very close for the $Au_{38}(SC2Ph)_{24}$ and $Au_{140}(SC2Ph)_{53}$ MPCs. (In fact, the second-order rate constants $k_{PE(I)}$ in Table 2 are near the ca. 1×10^{-2} M^{-1} s^{-1} rate constant determined for Au_{314} MPC,[10] although the ligands employed were different.) This leads to the important conclusion that the exchange kinetics of the first population (Phase I) of exchanging ligands are almost independent of the nanoparticle core dimension. That is, the (early) ligand exchange is not a size-dependent property, despite the facts that (a) the $Au_{38}(SC2Ph)_{24}$ MPC is definitely molecule-like and exhibits a substantial HOMO−LUMO gap energy,[26] whereas (b) any HOMO−LUMO gap energy for $Au_{140}(SC2Ph)_{53}$ MPCs is less than the one-electron energy increments (0.2−0.3 eV) of quantized double layer charging.[25] Theoretical studies[29b] predict that Au 4f binding energies for vertex sites on Au_{38}, while lower than for edge and terrace-like sites, are only about 10% lower than vertex sites on Au_{140}. In this regard, theory and experiment seem consistent.

Our earliest[10] analysis of ligand exchange on Au_{314} MPCs assigned the initial, faster stage of the reaction to ligands on vertex sites of the Au nanocrystal (see Scheme 1 of ref 10) and later, slower steps to reactions of ligands on edge and then on even slower terrace-like sites. This view has basis in the classical understanding[30] of exchange reactivity on flat metal surfaces having various kinds of defect sites thought to be more reactive. Defect sites include geometric features such as step edges and grain boundaries, as well as edges of monolayer ordered domains as discussed by Chidsey et al.[30d] The in-coming and initial monolayer thiolate ligands also have decided influence on the extent of exchange. For example, about $^1/_3$ of alkanethiolate monolayers on flat Au surfaces can be exchanged[30a,d] by alkanethiols, but the rest are resistant to exchange, whereas naphthalenethiolate monolayers can be completely exchanged by alkanethiols.[30b] Pyrenethiolate monolayers[30g] on 4 nm Au MPCs are completely exchanged by alkanethiols, whereas only a few percent of butanethiolate monolayer ligands are exchanged by a disulfide.[35] Nonetheless, for a given ligand, it is expected that its exchange reactivity would be greatest at defect-like sites.

We propose that the earliest stages of ligand exchange on $Au_{38}(SC2Ph)_{24}$ MPCs also involve ligands on vertex sites. Further, as noted in the Introduction, the fraction of the surface atom population on Au_{38} versus Au_{140} nanocrystals corresponding to defect (vertex plus edge) sites is far larger on the former nanoparticle. The ensuing expectation is that ligand binding dynamics on a Au_{38} core should be less dispersive (i.e., less varied) than on Au_{140}; this expectation is fully consistent with the serial-reaction, Phase I versus Phase II behavior described in Figure 3. Phase I rate constants for Au_{38} and Au_{140} are similar; the reactions occur on the same (vertex) kind of core site. Phase II reactions are slower for Au_{140}, being for ligands on edge and terrace-like sites, than on Au_{38} cores where the remaining ligand sites are on or are neighbors of vertex atoms.

The Phase I second-order rate constants in Table 2 show a definite substituent effect for both $Au_{38}(SC2Ph)_{24}$ and $Au_{140}(SC2Ph)_{53}$ MPCs. It is most noticeable that the polar, electron-withdrawing NO_2 substituent provokes a substantially faster ligand exchange. Results for $Au_{140}(SC2Ph)_{53}$ MPCs gave a well-formed Hammett substituent plot as shown previously.[31] The data for $Au_{38}(SC2Ph)_{24}$ MPCs are presented as a Hammett plot in Figure 5a, using standard σ substituent values.[38] The $Au_{38}(SC2Ph)_{24}$ plot is not as organized as the previous[31] $Au_{140}(SC2Ph)_{53}$ data, but the rate constants that we most carefully assessed, X = NO_2, Br, and CH_3, give a linear segment with slope of 0.86. The comparable Hammett slope, 0.44, for $Au_{140}(SC2Ph)_{53}$ MPCs was[31] also positive. We will return to a further consideration of the substituent effect below.

The Reverse Ligand Exchange Reaction. The nearly complete ligand exchanges accomplished for $Au_{38}(SC2Ph)_{24}$ MPCs yield Au_{38} core MPCs with different monolayers: according to the NMR analysis, $Au_{38}(SPhNO_2)_{24}$, $Au_{38}(SPhBr)_{22}(SC2Ph)_2$, and $Au_{38}(SPhCH_3)_{22}(SC2Ph)_2$. (See Supporting Information Figure S-6 for the ^1H NMR spectrum of $Au_{38}(SPhNO_2)_{24}$.) The new MPCS were isolated from large-scale exchange reactions. That the Au_{38} core is preserved after exchange is supported by preservation of the pattern of

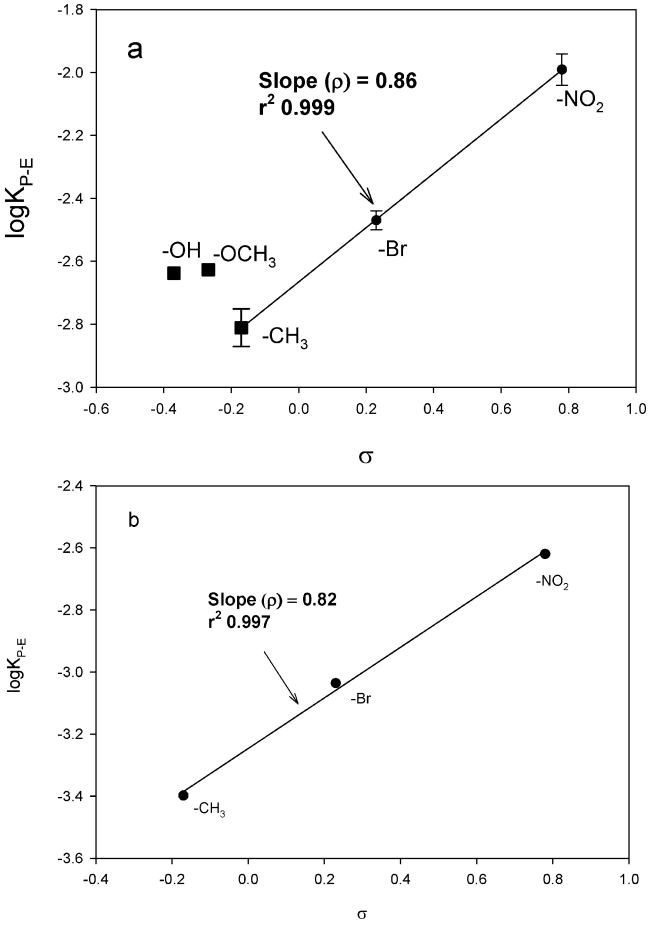

Figure 5. (Panel a) Hammett plot of $k_{PE(I)}$ rate constants for ligand place exchange reactions of $Au_{38}(SC2Ph)_{24}$ against standard substituent parameters, σ, for $-NO_2$; $-Br$; $-CH_3$; $-OCH_3$; $-OH$. (Panel b) Hammett plot for the reverse ligand exchange reaction.

Table 3. Second-Order Rate Constants for the Reverse Ligand Exchange Reaction: $Au_{38}(SPh-X)_{24} + m$PhC2SH → $Au_{38}(SC2Ph)_m(SPh-X)_{24-m} + m$HS−Ph−X

MPCs	PhC2SH/SPh–X[a]	$k_{PE(I)}$ (10^{-3} M^{-1} s^{-1})	$K_{EQ,PE}$[b]
$Au_{38}(SPhNO_2)_{24}$	2.2:1	2.4	4.2
$Au_{38}(SPhBr)_{22}(SC2Ph)_2$	6.0:1	0.92	3.7
$Au_{38}(SPhCH_3)_{22}(SC2Ph)_2$	7.3:1	0.40	4.0

[a] The relative number of moles of in-coming phenylethanethiol and the original thiolates in the monolayers of $Au_{38}(SPhX)_{24}$ MPCs. [b] Ratio of $k_{PE(I)forward}$ from Table 2 versus $k_{PE(I)reverse}$ from Table 3.

electrochemical reactions and associated energy gap seen[26] for the $Au_{38}(SC2Ph)_{24}$ MPC, as will be reported elsewhere.[39]

The fully exchanged MPCs open the door to study the reverse ligand exchange reaction, where $Au_{38}(SPhX)_{24}$ MPCs are reacted with phenylethanethiol:

$$Au_{38}(SPhX)_{24} + m\text{PhC2SH} \rightarrow Au_{38}(SC2Ph)_m(SPhX)_{24-m} + m\text{HSPhX} \quad (1)$$

The reaction was followed by monitoring the growth of the S−*H* resonance of the *p*-substituted arylthiol, HSPhX, liberated from $Au_{38}(SPhX)_{24}$. The early part of the reverse reaction is again first-order; Table 3 gives the associated second-order rate constants for X = NO_2, Br, and CH_3. There is again an obvious substituent effect on the exchange dynamics; the rate constants are $k_{PE(NO2)} > k_{PE(Br)} > k_{PE(CH3)}$. The Hammett plot of these results in Figure 5b has remarkably a slope, 0.82, that is nearly identical to that for the same substituents in Figure 5a (0.86). That the same substituent effect appears in both the forward and the reverse exchange reactions strongly supports our proposal that the reaction is an associative process. Additionally, in discussion of the substituent effect in the ligand exchange[31] for $Au_{140}(SC2Ph)_{53}$ MPCs, we noted that, classically, it is an indicator of how electronic effects of substituents affect charge distribution in the transition state. Lowering of the reaction's activation barrier for electron-withdrawing substituents (e.g., $-NO_2$) implies stabilizing of a buildup of negative charge taking place on the sulfur atom (or positive charge on the Au atom to which it is bonded) in the rate-determining step. Observation of the same substituent effect in both directions of the exchange reaction, that is, Figure 5a and b, further implies a concurrent bonding of both in-coming and leaving ligands to the Au core in the rate-determining step.

The $k_{PE(I)}$ forward (Table 2) and reverse (Table 3) ligand exchange rate constants refer to exchanges of the faster-reacting ligand population, which we postulate is that on the MPC core vertices. The equilibrium constant $K_{EQ,PE}$ for exchanges of phenylethanethiolate ligands with those of the three *p*-substituted arylthiols at those core sites is the ratio[40] of the forward and reverse rate constants, as given in Table 3. Remarkably, there is little variation among the $K_{EQ,PE}$ results; the average is 4.0 ± 0.3. That is, $K_{EQ,PE}$ lacks an evident substituent effect, implying that the reaction free energy for replacement of phenylethanethiolate ligands with −SPhX ligands is constant, and that bonding of −SPhX ligands at the vertex sites is more stable than phenylethanethiolate bonding by ca. 3.4 kJ/mol (or 0.035 eV/MPC). The difference is not large and is consistent with the analysis of Schlenoff et al.,[30b] which calls them "similar". That there is a thermodynamic stabilization of MPC bonding of a Au−SPhX moiety relative to that of Au−S$(CH_2)_2$Ph, that is more or less independent of "X", further implies that the difference in the Au−thiolate bonding energies lies in alkyl (i.e., $-SCH_2CH_2Ph$) versus aryl (−SPhX) bonding to the sulfur. A related implication is that the activation energy barrier for ligand exchange on Au_{38} vertices depends on substituents ("X") whereas the bonding strength ($K_{EQ,PE}$) does not. This is consistent with the activation model presented above.

Acknowledgment. This research was supported by grants from the National Science Foundation and Office of Naval Research.

Supporting Information Available: ^{1}H NMR spectra and further reaction profile plots. This material is available free of charge via the Internet at http://pubs.acs.org.

JA044638C

(39) Guo, R.; Murray, R. W., manuscript in preparation.

(40) The values of $k_{PE(I)}$ are initial rate constants and are taken at sufficiently large excesses of in-coming ligand that consideration of back-reaction rates is not necessary.